PERGAMON

Pattern Recognition 34 (2001) 255–270

PATTERN RECOGNITION
THE JOURNAL OF THE PATTERN RECOGNITION SOCIETY

www.elsevier.com/locate/patcog

A cost-effective fingerprint recognition system for use with low-quality prints and damaged fingertips

A.J. Willis*, L. Myers

Dept. Electrical Engineering, University of Witwatersrand, P. Bag 3, PO WITS 2050, Johannesburg, South Africa

Abstract

The development of a robust algorithm allowing good recognition of low-quality fingerprints with inexpensive hardware is investigated. A threshold FFT approach is developed to simultaneously smooth and enhance poor quality images derived from a database of imperfect prints. Features are extracted from the enhanced images using a number of approaches including a novel wedge ring overlay minutia detector that is particularly robust to imperfections. Finally, a number of neural net and statistically based classifiers are evaluated for the recognition task. Results for various combinations of the process are presented and discussed with regard to their utility in such a system. © 2000 Pattern Recognition Society. Published by Elsevier Science Ltd. All rights reserved.

Keywords: Fingerprint; Recognition; Enhancement; Classification

1. Introduction

Fingerprints are imprints or impressions of patterns formed by friction ridges of the skin in the fingers and thumbs. The uniqueness of such patterns was recognised by past cultures and their use as a means of personal identification has been in existence as early as the third century B.C. The ability to confirm the identity of crime suspects and to learn the identity of unknown felons from prints left at the scene of a crime is of obvious benefit to society. Thus, it is not surprising that law enforcement agencies are the ones to have made the greatest advances in techniques and equipment in use of fingerprints for positive identification. Closely allied with the art of criminal apprehension, human fingerprints can provide an unequalled method of personal identification for various other applications. These include security or access control systems, banking and credit systems and forensic or surveillance systems.

A shortcoming with many of the existing recognition techniques is that they all require a reasonable standard of input image. Many sophisticated fingerprint enhancement algorithms do exist [1–3]. However, these techniques are suited for police work, where processing time does not have to be within 1 or 2 s. Thus for a low quality, cheap, fast commercial system there is abundant room for improvement. Coetzee and Botha [4] have investigated this problem with reasonable success. They proposed a recursive line following binarisation and smoothing pre-processing, followed by feature extraction using a Fourier wedge-ring detector which detects minutia which manifest themselves as small deviations from the dominant spatial frequency of the ridges.

A further complication which has not yet been addressed is that of "bad" prints. This refers to fingerprints where the distinguishing patterns are unclear. This may be the result of one of several situations. As one gets older, one's fingerprints tend to wear very quickly and the definition between valleys and ridges significantly deteriorates. Elderly people's ability to replace the cells that build up this definition diminishes, with the result that their fingerprint patterns are difficult to obtain. Manual workers, particularly in rural and mining areas, subject their fingertips to severe punishment, resulting in

* Corresponding author. Present address: GE Harris Energy Control Systems, 4525 Manilla Rd SE, Calgary AB, Canada T2G 4B6. Tel.: + 1-403-214-4758; fax: + 1-403-287-7946.

E-mail address: ajwillis@home.com (A.J. Willis).

PII: S0031-3203(00)00003-0

injuries, scars, calluses and false grooves. All of these contribute to false minutia. Additionally, any system must be robust to people who obtain temporary cuts. Finally, some recognition algorithms are hindered by fingers with significantly different ridge thicknesses both within and between different fingerprints. Combining both low-quality images with low-quality prints, to facilitate a cheap and efficient commercial recognition system, presents a serious challenge. This is the problem that is addressed in this paper.

The noise in fingerprint images is highly correlated and often the statistics of such noises are unknown. Although noise covariance may be estimated or assumed to be Markov spatially, it is not unreasonable to expect that probabilistic noise reduction approaches will not work very well. A better alternative to the statistical approach would be a problem specific technique and thus an efficient fingerprint specific enhancement procedure has been developed. Both binarisation and line thinning are considered and efficiently dealt with. The large amount of false minutia generated may be dealt with in two ways. Xiao and Raafat [5] proposed a post-processing, minutia purification stage to eliminate spurious minutia. This is a costly procedure time-wise and therefore impractical for the problem.

A far simpler, more efficient post-processing procedure is suggested and tested. The other approach, which is the main focus of this paper, is to use the total image (or a robust representation thereof) to find a match. Thus, a rotationally and translationally invariant description of the entire fingerprint (perhaps with emphasis on minutia) is required for recognition purposes. Standard probabilistic classifiers, neural network classifiers and the newer probabilistic neural network are compared and their performance at the task at hand is evaluated.

2. Data generation

Many techniques of obtaining digital fingerprint images for identification applications exist. These may be loosely divided into inking and optical methods.

A large number of optical methods exist. These may briefly be divided into prism, holographic and laser systems. The basic principle of operation is uniform for all these methods and thus the prism method was selected due to its low cost and easy availability.

The prism method operates on the principle of total internal reflection and uses the configuration shown in Fig. 1. This consists of a prism placed in front of a CCD (charge coupled device) camera which is connected to a frame grabber card installed on a personal computer. The user places a finger on the longest face of the prism and parallel incoming rays of light passed through a diffuser for uniform brightness enter from one of the other sides of the prism. These rays are refracted differently depending on whether a point of contact of the finger with the prism (corresponding to a ridge), or a point of non-contact (a valley) was encountered. Total internal reflection will only occur where the ridges do not make contact with the prism surface. Thus, a pattern of bright and dark ridges appear on the third surface of the prism and these may easily be focused and captured by the camera system.

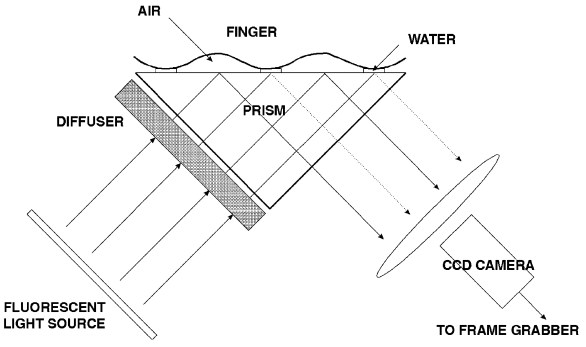

Fig. 1. Optical prism data generation method.

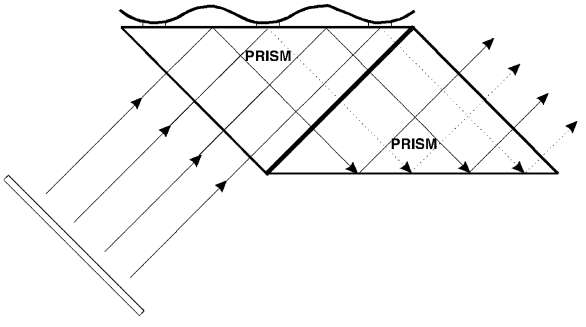

Fig. 2. The use of two prisms compensate for trapezoidal distortion. Note that all the rays of light that traverse the inside of both prisms are equal in length.

Compensation is necessary for the resulting deformation that occurs due to the fact that a finger is located obliquely to the optical axis and hence not at a constant distance from the camera lens. This is known as trapezoidal distortion. This deformation may be accounted for and corrected at the pre-processing stage by the software component of the system. This will however unnecessarily burden the operation time and thus the distortion should be corrected by the hardware component. To do this a second prism was used to rotate the reflection surface by an equivalent amount, but in the opposite direction with regard to the normal of the optical axis. This is schematically shown in Fig. 2.

2.1. Database

The database of prints used in the following experiments consisted of a set of 200 prints in total. This was

divided into 30 different fingers, with 6 images per finger. A further 10 prints were duplicate prints, but which were rotated at a spectrum of angles and the final 10 prints were duplicate prints which had obtained cuts not originally present in the original set. The prints had a wide variety of differing ridge thicknesses and consisted of "good" fingerprints, damaged fingerprints and those prints of elderly people. An example is shown in Fig. 3.

3. Image enhancement

The quality of a fingerprint image that is obtained using the optical, prism method contains serious degradation's. Image quality is poor due to non-perfect or non-uniform contact of the finger with the prism surface. This causes breaks in the ridges, bridges between ridges and overall grey-scale intensity variations. Furthermore, a poor contrast with a highly noisy background exists. In addition, the dirt and oil left behind by previous prints further negatively affects the print quality. In elderly people the lack of high ridge-valley definition causes a very poor quality (see Fig. 3) print to appear. This again is partly due to the nature of the optical generation method, whereby a good ridge-valley definition is required to produce a good quality image. These problems must be dealt with before recognition can be successfully performed.

Many standard and fingerprint specific image enhancement techniques are available for use with the problem at hand [1–8]. These techniques were tested on our database of prints and none were found to be adequate enough. The techniques of O'Gorman and Nickerson [2], Methre and Sherlock [1,2] were indeed effective but were discarded as they are designed for use with police work and thus the required processing time is too high for a small, fast commercial system. Gabor filtering was also considered but found to be complicated as compared to Fourier enhancement, since the selection of filters is image dependent and the computation of coefficients is difficult, as the Gabor functions are non-orthogonal. Thus, a method which operated in a similar manner to these, but which is far quicker was required. The basic principle of operation in these techniques was to divide the image into small processing blocks, create a specific filter for each block based on the average ridge direction and then to filter each block. Thus, a system which spontaneously creates a filter attuned to the exact direction is required. Directional information of a specific block is contained in the magnitude of the Fourier transform of that block. Thus if a block which contains two or three roughly parallel ridges is considered and the Fourier transform is taken, then it is presumed that the dominant frequencies of that block correspond to the ridges in the block. The Fourier transform may be computed according to

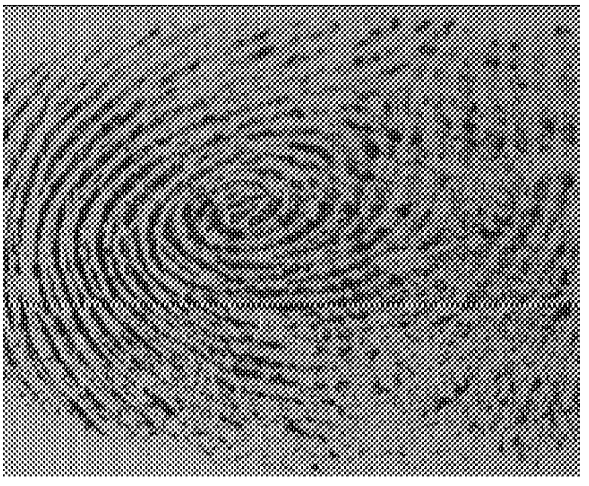

Fig. 3. Typical poor quality fingerprint.

$$F(u,v) = \sum_{x=0}^{M-1} \sum_{y=0}^{N-1} f(x,y) \exp\left\{-\mathrm{j}2\pi\left(\frac{ux}{M} + \frac{vy}{N}\right)\right\} \quad (3.1)$$

for $u = 0, 1, 2, \ldots, M-1$ and $v = 0, 1, 2, \ldots, N-1$,

In order to enhance a specific block by its dominant frequencies, thereby thickening ridges and more finely separating parallel ridges, it is possible to multiply the FFT of the block by it's magnitude a set number of times. When the inverse FFT is computed, it is found that the block is indeed enhanced. This is best illustrated graphically as follows. Fig. 4 is the block that requires enhancement. The FFT of the block is computed according to Eq. (3.1). Next, the magnitude of the FFT is taken, this is multiplied by the original FFT and the inverse Fourier transform is computed. This is done with the following equation:

$$f(x,y) = \frac{1}{MN} \sum_{u=0}^{M-1} \sum_{v=0}^{N-1} F(u,v) \exp\left\{\mathrm{j}2\pi\left(\frac{ux}{M} + \frac{vy}{N}\right)\right\} \quad (3.2)$$

for $x = 0, 1, 2, \ldots, M-1$ and $y = 0, 1, 2, \ldots, N-1$.

The result is depicted in Fig. 5. It may be seen that the ridges are indeed made solid and well separated as required. If the magnitude of the FFT were squared or cubed and then multiplied, an even better result would be obtained as depicted in Fig. 6. If the block under consideration contains a minutia such as in Fig. 7, the results are somewhat different.

Fig. 8 shows the consequences of multiplying by the magnitude of the FFT twice. It may be seen that since the branch which forms the minutia differs from the dominant direction of the block, it becomes obscured, indicating that slightly less enhancement ought to be applied. This may be done in the following manner.

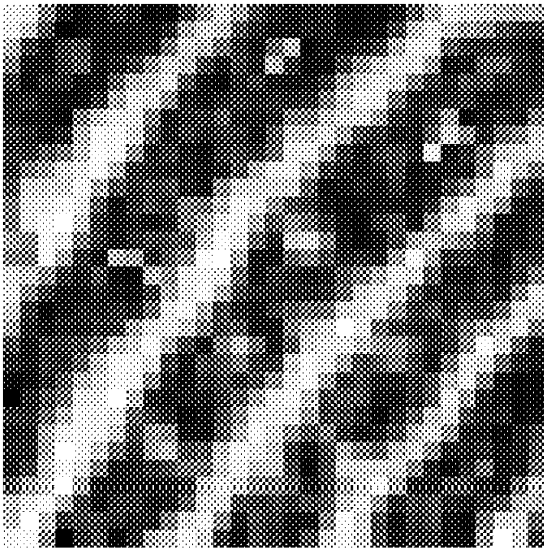

Fig. 4. Arbitrary block that requires enhancement.

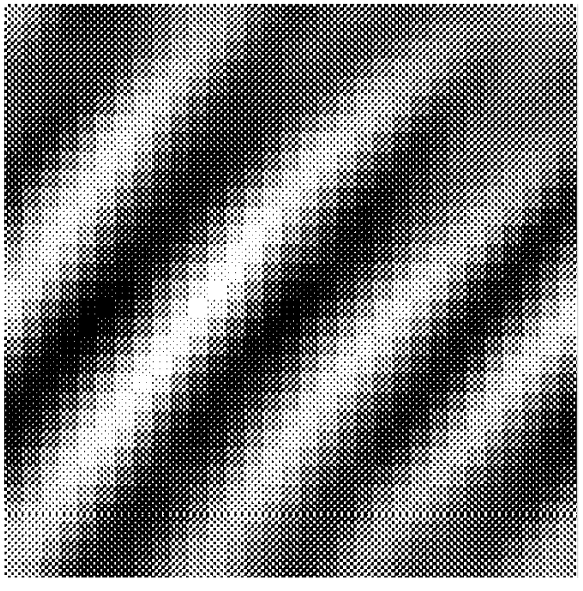

Fig. 5. Fingerprint block enhanced by one multiplication of FFT magnitude.

Rather than multiplying by whole factors of FFT magnitudes, a fraction or power of the magnitude should be used, i.e.

$$g(x, y) = F^{-1}\{F(u, v) \times |F(u, v)|^k\}, \tag{3.3}$$

where $g(x, y)$ is the enhanced block and 'k' is an experimentally determined constant, which is between one and two.

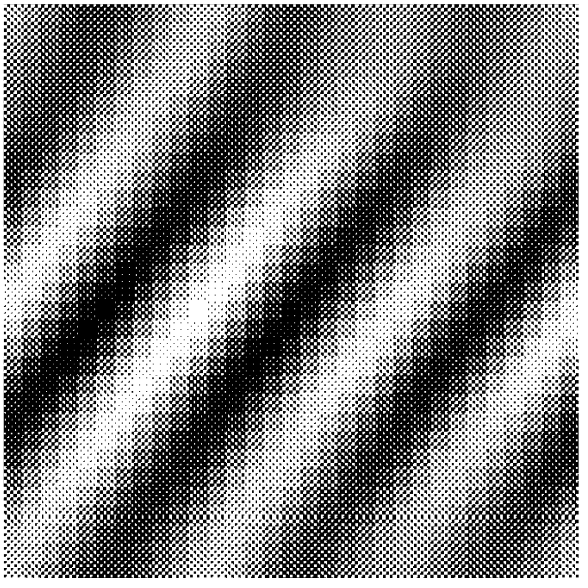

Fig. 6. Fingerprint block enhanced by two multiplications of FFT magnitude.

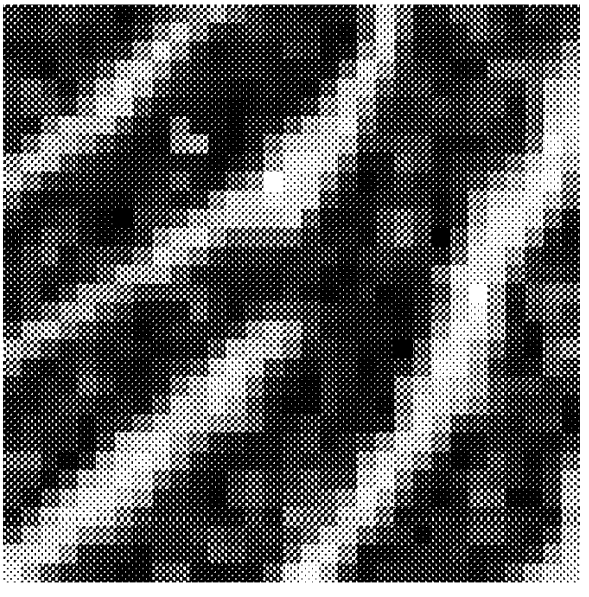

Fig. 7. Unenhanced fingerprint block containing minutia.

The results of $k = 1.2$, 1.4 and 1.7 are shown in Figs. 9(a), (b) and (c), respectively. Thus it may be seen that for $k = 1.4$ a good trade off between ridge enhancement and block direction is obtained.

From the above reasoning, it is clear that the requirements of patching in holes and smoothing, as well as

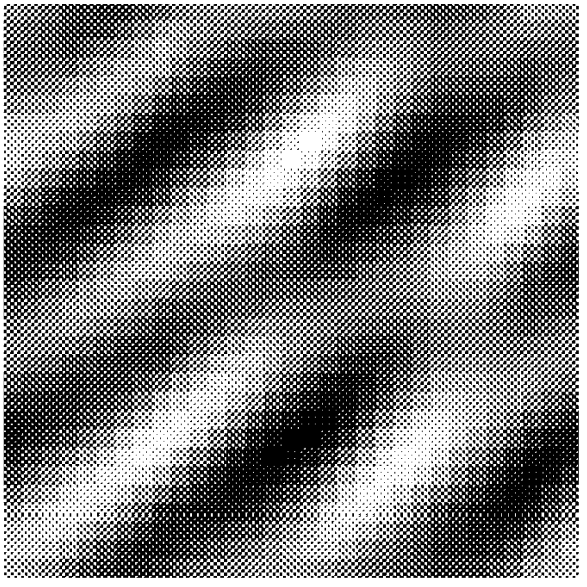

Fig. 8. Fingerprint block containing minutia that is enhanced by two magnitude FFT multiplications.

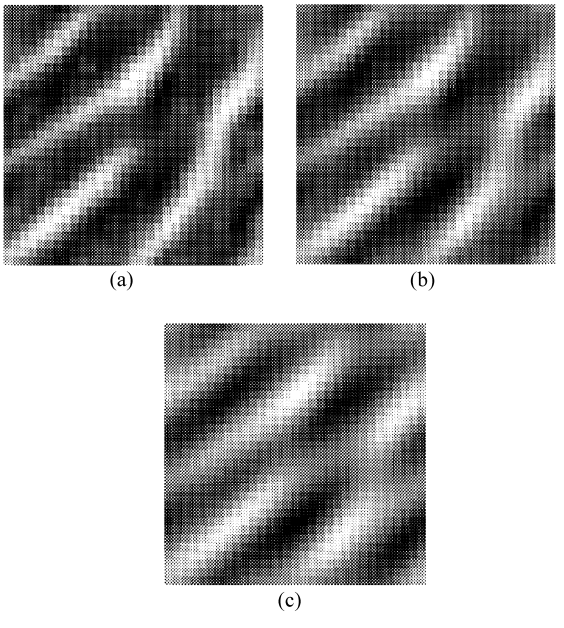

Fig. 9. Results of enhancing a fingerprint block containing a minutia for $k = 1.2$ (a), $k = 1.4$ (b) and $k = 1.7$ (c). It may be seen that $k = 1.4$ is the optimal trade off.

separating incorrectly joined ridges is met. Furthermore, this method is especially well suited to areas which have extremely low contrast, as illustrated in Figs. 10(a) and (b). This is because the ridge information in these areas is

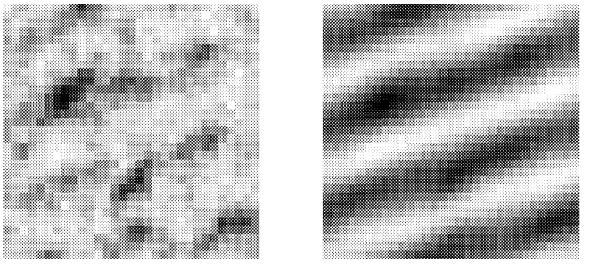

Fig. 10. Low contrast, low pressure block (elderly person's print) (a) and the resultant FFT magnitude enhancement (b).

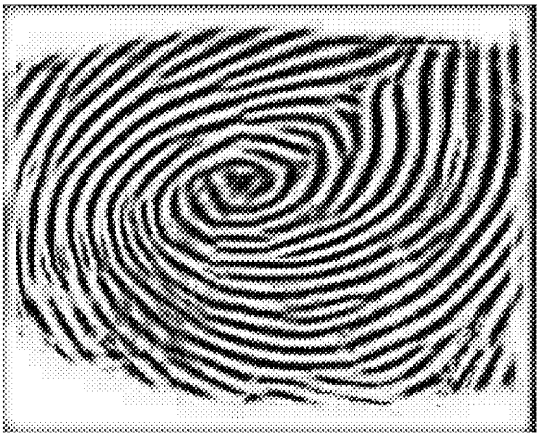

Fig. 11. Final FFT enhancement of fingerprint image.

still contained in the FFT. In areas where some of the ridge is missing, the algorithm may be seen to "predict" what it should look like, based on other information in the block.

From experimentation a block size of 32×32 pixels was found to be best as in the average print it contains three or four ridges and using a fast radix-2 FFT when the block size is a power of two, the FFT speed is optimum. Note that no serious error is incurred for small fingerprints such as that of children, as the block ridge frequency is not critical to the algorithm.

Applying this algorithm causes two problems to occur. The first is at the edges of adjacent blocks. This edge effect may easily be compensated by overlapping blocks. An overlap of 24 pixels was found to be optimum in successfully removing this edge effect. The second problem occurs at the edges and background of the image. This too is easily compensated for by summing the grey level pixels in each block and if this sum exceeds a threshold, then the block is assigned to the background. If the sum indicates that the block contains both the edge of the print and actual background, it is thresholded to a binary

image before the FFTs are computed. The final result of the corrected algorithm applied to the typical low-quality print of Fig. 4 is shown in Fig. 11. Thus, it may clearly be seen that this type of enhancement does indeed work for the full spectrum of low-quality prints and low-quality images. The processing speed of this algorithm is also vastly superior as the need to determine an orientation image and then to select a correct filter is automatically done and therefore these steps are bypassed.

3.1. Binarisation and thinning

Many feature extractors operate best from a binary or thinned binary image. This is due to improved contrast and the fact that a binary image facilitates easier recognition of ridges and key features. In order to binarise the image, a clean, well-defined grey-scale image is required. If one were to binarise the noisy grey-scale image, it would be impossible to recover the necessary information to facilitate efficient recognition of the print.

Two main types of binarisation algorithms exist, global and local binarisation. No noticeable difference was noted when using each type of binarisation and thus the global method was selected due to its faster computational speed. The actual threshold used was chosen according to Brink's correlation threshold algorithm [9].

The skeleton of a digital figure can often be regarded as a convenient alternative to the figure itself. The skeleton or thin-line representation of a fingerprint is perhaps closer to the human conception of the fingerprint pattern and therefore it should be more amenable to extraction of critical features, especially minutia extraction.

Many thinning algorithms were reviewed and the most effective with regard to speed and accuracy was that of Chen and Hsu [10]. A sample of a thinned print is depicted in Fig. 12.

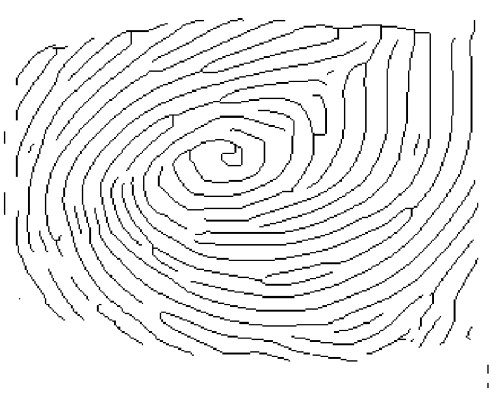

Fig. 12. Thinned binarised and enhanced print using the Chen and Hsu algorithm.

4. Feature extraction

Minutia are characteristics of a fingerprint that are useful for identification. They are essentially interruptions of the normal flow of the ridges such as ridge endings, bifurications, dots, short ridges, bridges, loops, crossovers and interruptions.

Many automatic recognition systems only consider ridge endings and bifurications as relevant minutia [11–13]. A reason for doing so is that it is more likely that bridge and island structures are due to false minutia and a large number of endings and bifurications are more than adequate for absolute recognition. An extra advantage may be obtained in a system that does not differentiate between these minutia. This is due to two possible situations. When a real bifurication is mistakenly separated, it becomes an end point with close to the same relative location and similarly if an end point mistakenly joins a ridge, a bifurication with the same relative location is formed. That is if no distinction is made between the types of minutia and only their positions are considered, no serious error is incurred. This is illustrated in Fig. 13.

The easiest and most accurate way of extracting minutia is from the thinned binary image. Leung et al. [7] propose a system which uses neural networks to locate bifurications in a print, whilst a few other systems Le Roux [14], and Weber [8] use line following ideas to locate other types of minutia. Since it is only required to find bifurications and end points, this is best done via use of the concept of *crossing number* [15]. Using this method, all valid bifurications and end-points are marked. At this stage it is necessary to eliminate false minutia. The main cause of false minutia occurs when thinning around a hole results in a pair of false bifurications. Other false minutia are false bridges and false tails. These three minutia are depicted in Fig. 14.

In general, it may be seen that all the false minutia have the common property of being joined to another minutia in a very short distance. If a minimum threshold distance is selected and all the lines originating from all the minutia are traced for that minimum distance, we may then eliminate those minutia that had lines that reached another minutia within the minimum distance. The problem that arises is how does one know that at least one of the minutia eliminated may in fact be a valid minutia. An example of this situation occurs when there is a valid bifurication that becomes a triangle due to a false bridge. All three minutia are accordingly deleted, when in fact one of them should have been retained. This problem is overcome due to the nature of the recognition algorithm and will be dealt with later. It should be noted that the above distance following procedure does eliminate far more false minutia than the few instances where real minutia are deleted.

Once the minutia are located it is required to find a reference point that will be in a similar (not necessarily

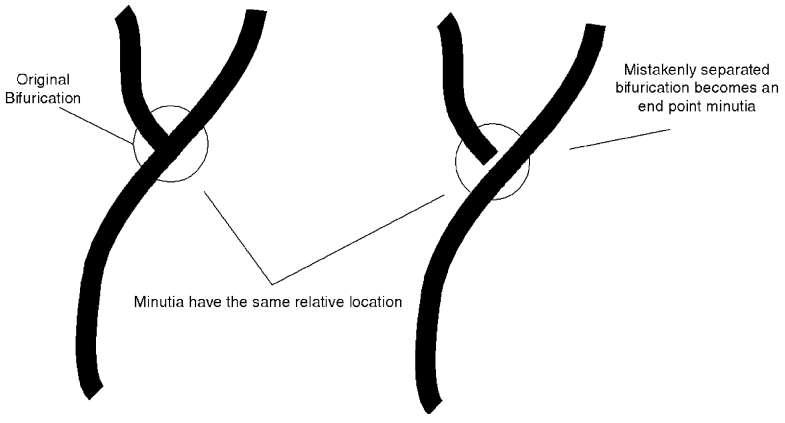

Fig. 13. Fingerprint minutia and their thinned versions, illustrating the fact that mistaken bifurications and end-points still result in minutia with the same relative locations.

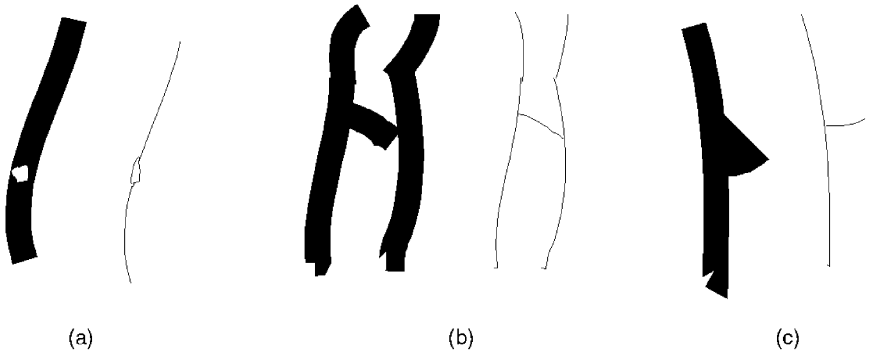

Fig. 14. Sections of binary prints and the corresponding thinned prints illustrating the formation of false minutia. (a) False pair of bifurications, (b) False bridge and (c) False tail.

identical) place each time the print is taken. This is done by computing a weighted centroid of all the minutia and the actual print. This is done by setting the value of all the minutia locations to five and the ridge pixels to one with the background as zeros and then computing the centroid coordinates. This may not be absolutely accurate, but as will be shown later this is not a crucial issue.

Once the reference point has been located a 'dart board' pattern of wedges and rings is overlaid on the image, with the centre of the board at the reference point. A target board grid with less than the typical number of segments is depicted in Fig. 15. The image is first padded with zeros to allow the board to fit. The number of minutia contained in each segment of the grid forms one element of the feature vector. Thus for a grid such as the one shown in Fig. 15, the resultant feature vector is

$$\left(\sum_{R1W1} m_i, \sum_{R1W2} m_i, \sum_{R1W3} m_i, \sum_{R1W4} m_i, \sum_{R2W1} m_i, \sum_{R2W2} m_i,\right.$$

$$\left.\sum_{R2W3} m_i, \sum_{R2W4} m\ i, \sum_{R3W1} m_i, \sum_{R3W2} m_i, \sum_{R3W3} m_i, \sum_{R3W4} m_i,\right),$$

where $\sum_X m_i$ is the number of minutia contained in segment X. The accuracy of the detector is affected or fine tuned by varying the number and size of the segments used. This also affects the dimension of the feature vector. The detector allows for rotational and translational invariance as if a small amount of translation or rotation is applied, roughly the same amount of minutia will fall into each segment as in the training print. The amount of invariance allowed may be controlled by the size of each segment. It is not likely that more than 15° of rotation will be present, given the guides on the hardware and common sense of the subjects applying their prints. In the tests presented here the rotation was within 15°, but if this was not the case the images can be aligned along the axes of symmetry using the Hoteling transform, which is based on a Kahunen Loeve decomposition.

The reference point is not too critical, as long as references for varying prints are within close proximity to each other. Our experience was that the changes in the feature vector were slowly varying enough on a scale introduced by operator error in selecting the same reference. An empirical procedure was used to determine the

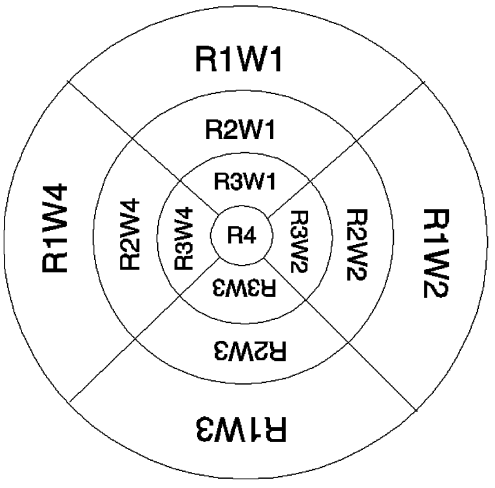

Fig. 15. Labelled minutia wedge-ring overlay.

optimum number and size of segments used. Although these numbers are application specific, it was found that the optimum numbers were 10 rings and 12 wedges.

The centre segment was chosen not to contain any wedges due to the slight variances of the references points. Furthermore, the fact that since there are often many more minutia close to the centre, adding wedges would place limits on the accuracy due to the rather small segments that would be created near the centre region. It was noted that most errors occurred in segments which erroneously contained a large number of minutia. In order to combat this a maximum limit was placed on the number of allowable minutia within a segment and any segments exceeding this maximum were simply thresholded to the maximum. The post-processing stage does eliminate most of these cases, however due to the positioning of fingers, sometimes false ends are created as the finger overlaps its boundaries when placed down. The post-processing procedure does not eliminate these false ends as they are well within the threshold distance of other minutia along ridge lines. The technique of using a maximum value allowed in any segment was also tested without first applying the post-processing. This was to determine if all the false minutia could be eliminated in this manner.

It is noted here that for classification, the smaller the dimension of the feature vector, the more optimal a given classifier's performance is. However, as one decreases the number of segments used, the accuracy of a classifier is diminished and thus a compromise between a large and a small amount of segments must be reached.

The minutia-detector operates on all the minutia present in the fingerprint image. If in one segment, either one or two minutia are missing or extra minutia are present, the performance of the whole detector should not be too adversely affected. It is for this reason that the system functions well in the presence of small temporary cuts and other disfigurements. A cut will create false minutia at each point that it crosses a fingerprint ridge, as well as at either end of the cut. This is enough false minutia to seriously hinder other recognition systems. Most of these spurious minutia will in fact be eliminated in the post processing procedure, as the bridges formed due to the cut are within close proximity of each other. Those incorrect minutia that remain after the post-processing, will not seriously affect the performance of the detector as the majority of segments will contain the correct number of minutia and as mentioned earlier, having one or two more minutia in a few segments still allows for correct recognition. In addition, the thresholding to a maximum number of minutia per segment ought to completely eliminate any errors incurred by false cuts. The problem of eliminating some true minutia, as mentioned earlier, is dealt with in the same fashion.

5. Transform feature extraction via spectral analysis

Since fingerprints are broadly composed of periodic structures (the ridges and valleys), it should be natural to examine them in the frequency domain in order to extract relevant features. Often the minutia in a fingerprint correspond to different spatial frequency components than the fingerprint ridges. The actual frequencies associated with the minutia should vary from print to print and it is this difference that may be exploited in order to extract meaningful information for classification purposes.

The fingerprint image is first transformed to the spatial frequency domain via the two dimensional Fourier transform (Eq. (3.1)). The power spectrum is more useful for feature extraction and may be obtained by squaring the magnitude of the transform. Features may then be extracted via a the wedge-ring classifier [4,16]. This is a well known technique, often used to give a statistical description of textures and to discriminate between them [17]. The features are formed by summing the spectral values in circular rings of varying radius r and constant thickness Δr, i.e.

$$\lambda_i(r) = \sum_u \sum_v |F(u, v)|^2, \tag{5.1}$$

where $r \leqslant (u^2 + v^2)^{1/2} \leqslant r + \Delta r$ and $0 \leqslant r \leqslant N/2$ and the maximum image dimension is N. The subscript i refers to the ith ring out of n rings. Wedge segments with varying orientation ϕ and segment width $\Delta\phi$ are also used, i.e.

$$\beta_j(\phi) = \sum_u \sum_v |F(u, v)|^2, \tag{5.2}$$

where $\phi \leqslant \arctan(v/u) \leqslant \phi + \Delta\phi$ and $0 \leqslant \phi + \Delta\phi$. The subscript j refers to the jth wedge of total m wedges. Since the power spectra of real functions are symmetrical, the

summations in Eqs. (5.1) and (5.2), need only extend over a half-plane of each power spectrum. The complete feature vector is thus given by

$$f = [\lambda_1, \lambda_2, \ldots, \lambda_n, \beta_1, \beta_2, \ldots, \beta_m]. \quad (5.3)$$

Each ring may be considered to represent a specific set of spatial frequencies, whilst each wedge represents the entire range of spatial frequencies across a specific range of rotation. This system thus represents a global description of the fingerprint and therefore should be fairly robust to small changes in prints, such as temporary cuts. It should also be particularly good with damaged and calloused prints, as the callouses and areas of damage contribute their own unique frequency components and these components are consistent for prints within the same class. Lastly, this system is completely invariant to translational differences, as the Fourier transform is always centred on the origin of the axis. The system is reasonably rotationally invariant as long as the number of wedges are kept reasonably small. A trade-off between the dimension of the feature vector and the accuracy of the detector exists and thus the number of wedges and rings have to be carefully and experimentally determined.

6. Feature classification

The final stage of the fingerprint recognition system is the classification of the relevant feature vectors. Thus, the task of the classifier is to assign an unknown feature vector to one of many known classes. Owing to the fact that each unique individual (whose prints represent one class) is previously known, only supervised learning paradigms were considered.

Many different classifiers were tested as previous work has often placed the emphasis on the feature extraction stage and then only considered one or two different classifiers. An attempt has been made here to test the performance of a large variety of classifiers in order to obtain an optimal performance. Some classifiers ideally work best with large amounts of training data, which is obviously unavailable in this situation. However, it is still possible to obtain a reasonably clear idea of which classifier/feature extraction combination will prove to be optimal. For more details on the classifiers used, consult Duda and Hart [18], Chen [19], and Specht [20].

The classifiers used along with their abbreviations for results figures, are:

- K-nearest-neighbour classifier (KNN).
- Weighted nearest-neighbour classifiers (WNN).
- Euclidean minimum distance classifier (EMD).
- Back-propagation neural network classifier (BP).
- Learning vector quantisation neural network classifier (LVQ).
- Radial basis function neural network classifier (RBF).
- Probabilistic neural network classifier (PNN).
- Correlation classifier (CCL).

7. Results

Many of the classifiers have variables or parameters which require optimisation, e.g. number of neurons, etc. Furthermore, the number of segments in the feature extractors also require optimisation. Thus, results presented here are for the already optimised classifier variables and only a few relevant feature extractor parameters are shown in order to indicate relevant trends. The numbers in the keys on the graphs indicate the number of prints used in the training stage. Most previous work has only used one print to train a system and here the performance of multiple training feature vectors is investigated. The results are shown in Figs. 16–23.

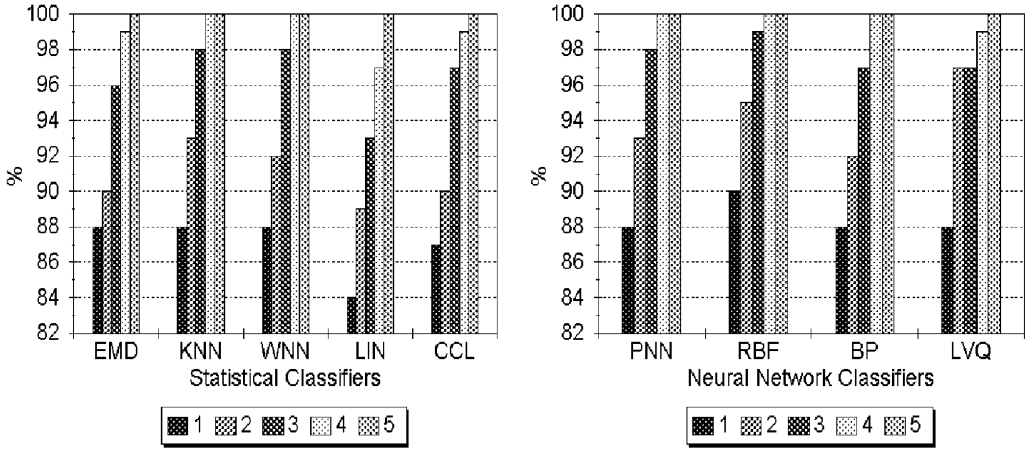

Fig. 16. Identification results for minutia-overlay features for 8 rings and 7 wedges.

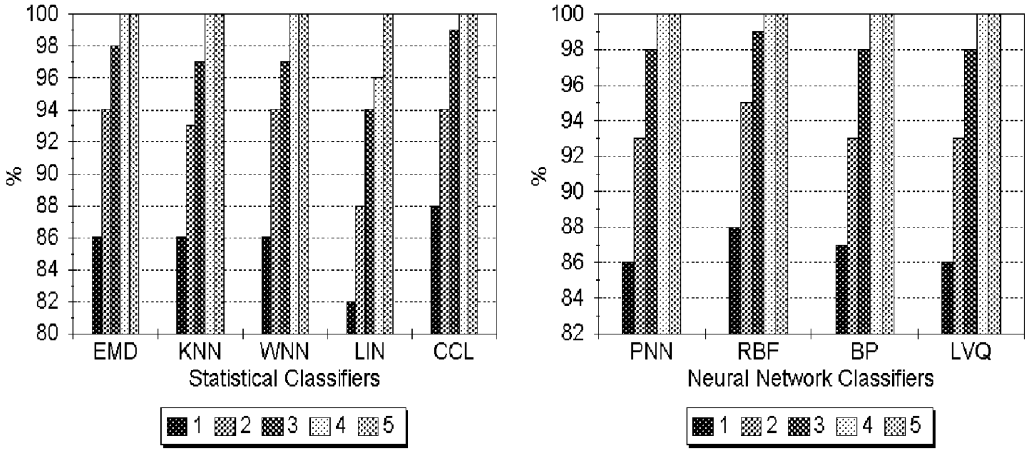

Fig. 17. Identification results for minutia-overlay features for 5 rings and 7 wedges.

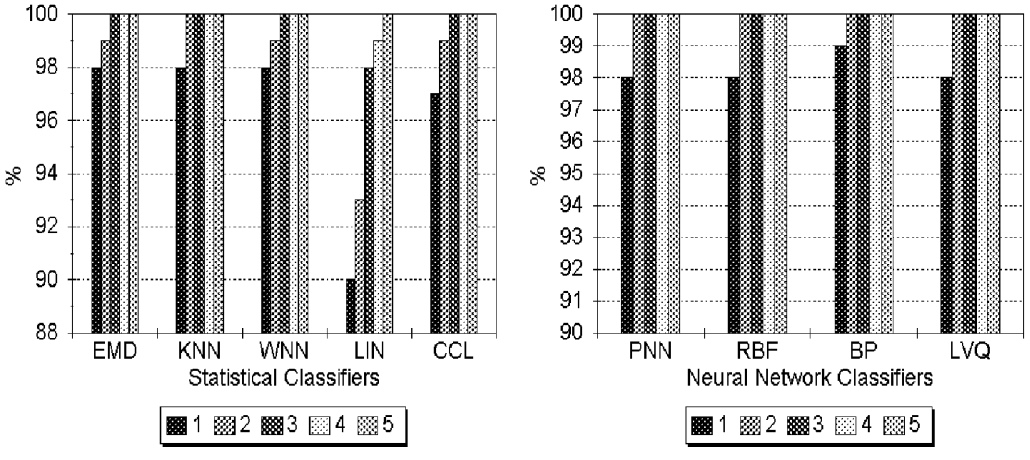

Fig. 18. Identification results for minutia-overlay features for 10 rings and 12 wedges.

The features extracted via minutia overlay require the number of rings and wedges to be optimised. The results here are shown for four different numbers of wedges and rings so that a trend can be discerned, but many more numbers were evaluated. As can be seen from Figs. 16–19 the best performance was found for 10 rings and 12 wedges. Hyndred percent recognition is achieved for only 2 training prints per class for most of the classifiers, but high performance still results with only 1 training print per class. Best performance occurs with a large number of rings and a small number of wedges. The latter seems to be critical and performance degrades quickly as the number of wedges increases (this may possibly be attributed to the rotations present in the images). The number of rings was not so important but 10 rings was found to give best performance. The best pattern was that of large spacings for the first and last two rings with the rest uniform. When post-processing was not included the best recognition was 62%.

In common with the minutae overlay approach, the Fourier transform feature extraction method also required the segment geometry to be optimised. This was done experimentally and the classifiers applied to produce the results shown in Figs. 20–23. Overall non-thinned binary images offered superior performance when using Fourier features. Grey-scale images performed remarkably well, which may be attributed to the greater number of frequency component contributions arising from varying grey-scale slopes. The original grey-scale images slightly out performed the enhanced ones, probably due to the holes and other fine structure that are smoothed in the enhanced print. These contrib-

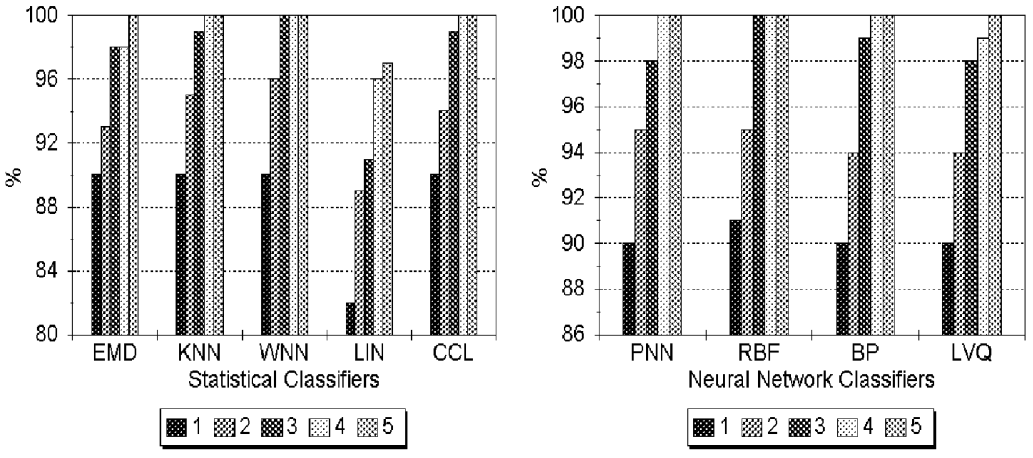

Fig. 19. Identification results for minutia-overlay features for 10 rings and 16 wedges.

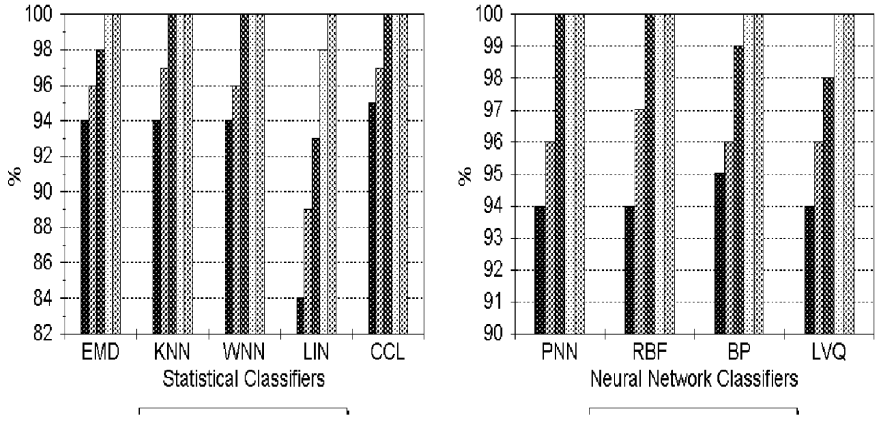

Fig. 20. Identification results for Fourier features extracted from the original grey-scale prints.

ute unique information that it appears is important in classification. The slightly different backgrounds did not hinder recognition performance. The Fourier features correctly identified prints with cuts and identified half of the rotated prints.

Correlation classification is shown in Fig. 24. Here the thresholds are shown over which the pixels of the normalised correlation were counted. Another approach is to select a certain number of pixels that should not be exceeded for a given threshold. The reasoning being that a good correlation peak is sharp and will yield few pixels above this limit. The threshold was experimentally determined and the best results shown as the 'Max' method. Cross-correlation performed well for thresholded binary prints, where extra ridge thicknesses allowed a wider variety of spatial shift tolerance.

The wavelet-based correlation classification made use of the discrete wavelet transform to produce details of the image at different resolution levels, j. These are then correlated to produce a classification. Resolution levels are obtained iteratively from the previous level using the à trous algorithm [21]. This algorithm uses a scaling function to build a low pass filter that is convolved with the image to transform it down one resolution level. A B spline of degree three was used for scaling. Only three levels ($j = 1$–3) was considered as beyond this the computational burden negates the objective of this work in producing a fast and simple system. Results are shown in Figs. 25–27. Wavelet correlation improved the recognition above that of simple cross-correlation with the best results occurring for scale $j = 2$ using binary prints.

To make an assessment of these results in terms of the objective of designing a cost effective system, the classifiers used need to be evaluated for storage capacity and processing time along with recognition performance. On

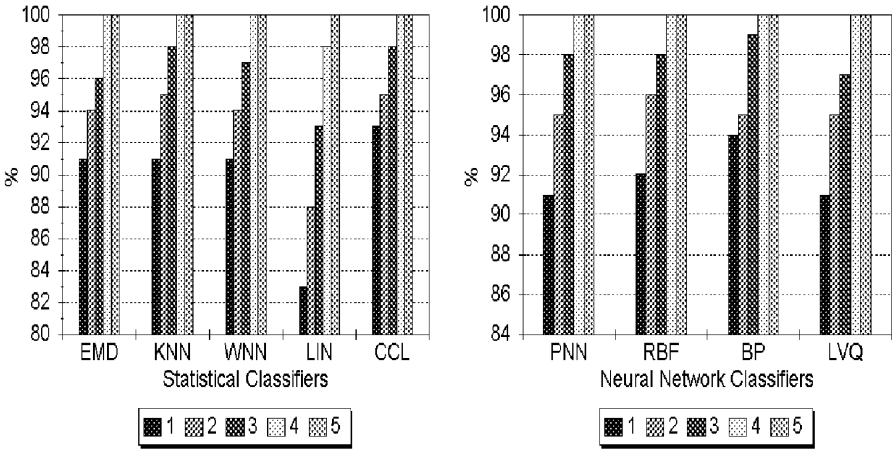

Fig. 21. Identification results for Fourier features extracted from the enhanced grey-scale prints.

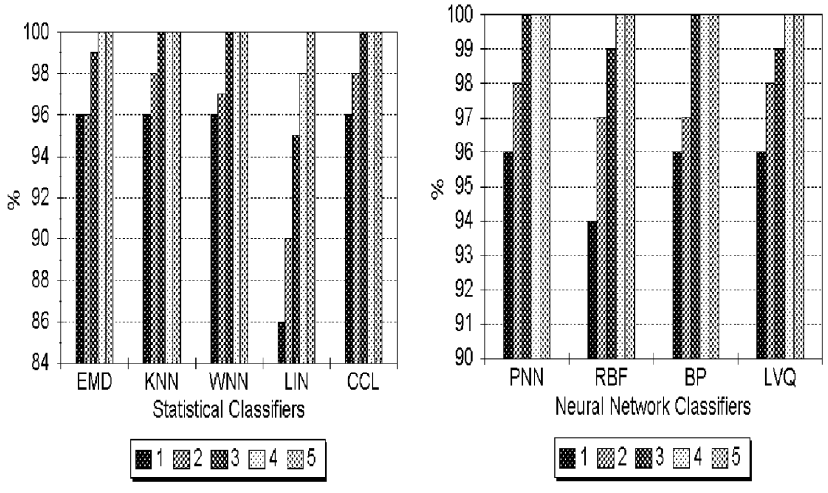

Fig. 22. Identification results for Fourier features extracted from the binary prints.

average the recognition performance of the neural net classifiers was better than their statistical counterparts. Specifically, the classifier performance was feature dependent, but back-propagation and probabilistic networks giving consistently good performance. Radial basis networks performed very well but were prone to give very poor performance on occasions. Of the statistical classifiers the nearest-neighbour derivatives gave best results, especially the first nearest neighbour, with weighted nearest neighbour offering no advantages. The poor performance of the linear classifier indicates that the features are probably not linearly separable. From the errors made it appeared that the LVQ network is behaving in a way that is similar to a combination of EMD and KNN classifiers, while the probabilistic classifier seemed to perform very much like the nearest neighbour. The correlation classifier performed surprisingly well, especially with transform features.

Classification times were dependent on the size of the training set and dimension of features. As the size increased the neural net classifiers obviously became comparatively faster. Of the statistical classifiers WNN and CCL were the slowest, while linear and EMD were fastest. Training times were not a consideration for the statistical classifiers but are important for the neural-net-based methods. For these classifiers the training times in order of fastest to slowest were radial basis networks, probabilistic networks, learning vector quantisation and back propagation. The latter is particularly cumbersome.

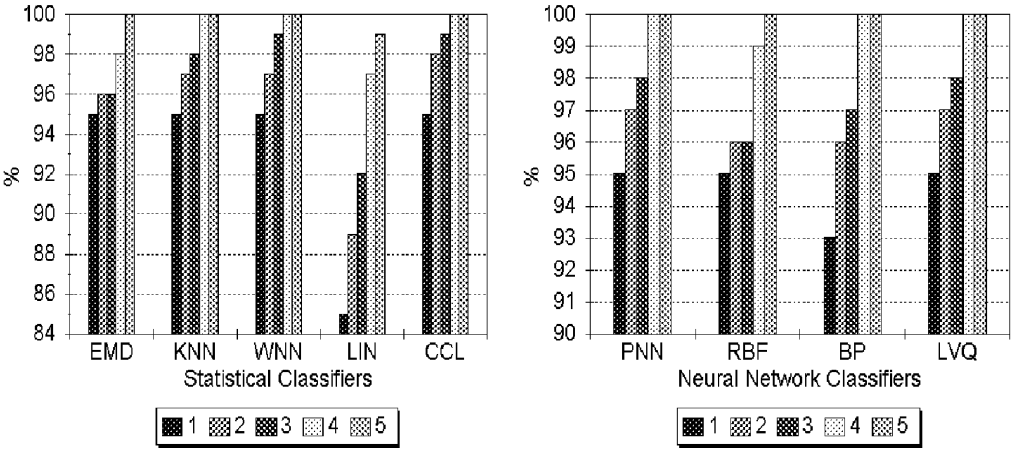

Fig. 23. Identification results for Fourier features extracted from the thinned binary prints.

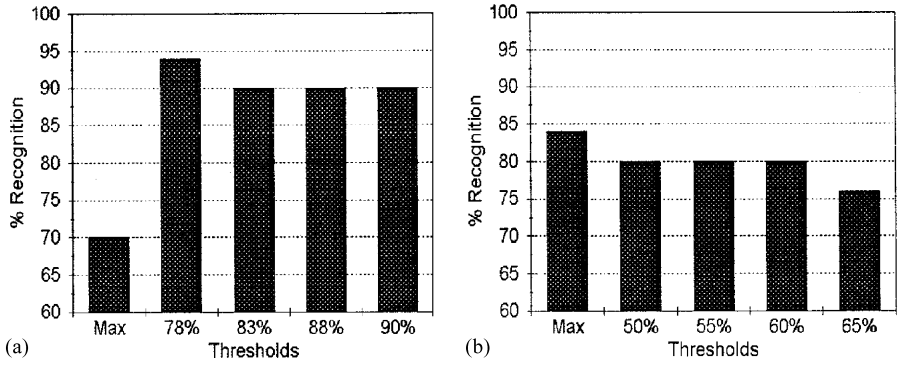

Fig. 24. Correlation classification for binary and thinned binary prints. (a) Binary. (b) Thinned.

8. Conclusions

A solution to the problem of a cost effective, efficient fingerprint recognition system for use with both low-quality prints and damaged fingertips was investigated. Many fingerprint systems are commercially available, but most of these are too expensive and have not been fully tested on damaged or elderly people's fingerprints.

Initially a database of the full spectrum of damaged, elderly people's and unusual fingerprints was required. The nature of the hardware used to obtain the fingerprint images rendered rather low-quality images. The cost of the hardware was, however, minimal and may be easily constructed. In most commercially available systems, it is the hardware component that renders the systems highly expensive. Unfortunately, the resulting loss in image clarity places a burden on the software component, which must cater for this.

An ideal recognition algorithm will provide perfect recognition on the original digitised print without any subsequent enhancement being applied. A few algorithms which attempted to do this were investigated. However for most algorithms, a large amount of enhancement needs to be applied. Many techniques were investigated and it was found that the best method for enhancement was to scan the image in overlapping blocks and to enhance each block by a percentage of its dominant spatial frequency. This information was contained in the magnitude of the Fourier spectrum of the block. This technique was particularly suited to images with very bad contrast, images where some sections hardly showed up and images with breaks and holes in the ridge structure. The computational burden of the enhancement is very small compared with many complex existing techniques. In some cases it was necessary to binarise and thin the enhanced image. This was achieved using a global threshold for binarisation and a simple parallel table mapping technique to thin the image. The thinning process was marginally speeded up by performing finishing checks only after a predetermined number of passes.

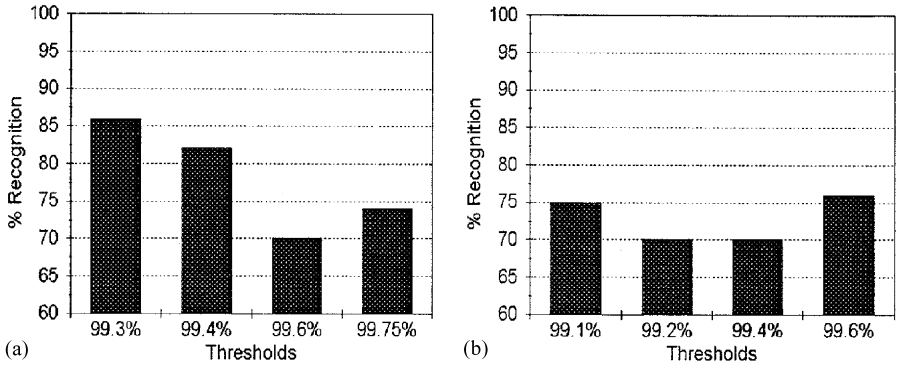

Fig. 25. Wavelet correlation classification results for binary and thinned binary prints $j = 1$. (a) Binary. (b) Thinned.

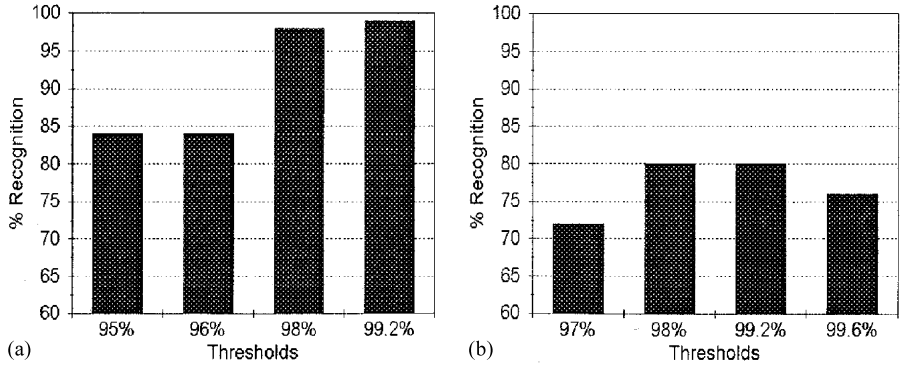

Fig. 26. Wavelet correlation classification results for binary and thinned binary prints $j = 2$. (a) Binary. (b) Thinned.

The minutia wedge-ring features provided the highest recognition accuracy for the lowest number of training prints and thus would be the only choice in applications where the number of available training prints is small. A minimum of two training prints per class was required. Unfortunately, this type of feature extractor requires the most processing time as it operates upon the thinned prints, further needing to identify minutia and then perform post-processing upon them. The computation time should not prove to be a serious concern if dedicated hardware is used for the system. This technique performed remarkably well for prints with temporary cuts and those that had small rotations. If a very fast processor is available, it may be worthwhile considering using the position standardisation technique prior to the use of the minutia overlay, as this ought to improve results.

Features extracted from the Fourier domain by summing circular and radial segments were found to perform fairly well. This technique is best suited for use on the binary image. It was found that 100% performance could be achieved with a minimum of three training prints per class. Since this technique also operates relatively well from the unenhanced print, and it requires very little processing time, it is quite a suitable technique to use. In fact due to its minimal processing time, it could be used in conjunction with other techniques to provide a more robust system. If this were the case, perhaps less than three training prints per class could be used, as the performance for one and two training prints per class was still over 95%. These features are fairly robust to rotation and temporary cuts.

The performance of different classifiers were investigated in order to select an optimal classifier. There is however no universal optimal classifier and the results largely depend on the particular task at hand. Furthermore, there is little variation in the performance of most classifiers and thus the criterion used to select a classifier would very much depend on the time and storage requirements of the particular application. In general, the neural network classifiers provide the best performance in terms of these two criteria and should be used unless for some reason on-line training and updating is required. A system might require to increase its performance every time a positive identification is made, by

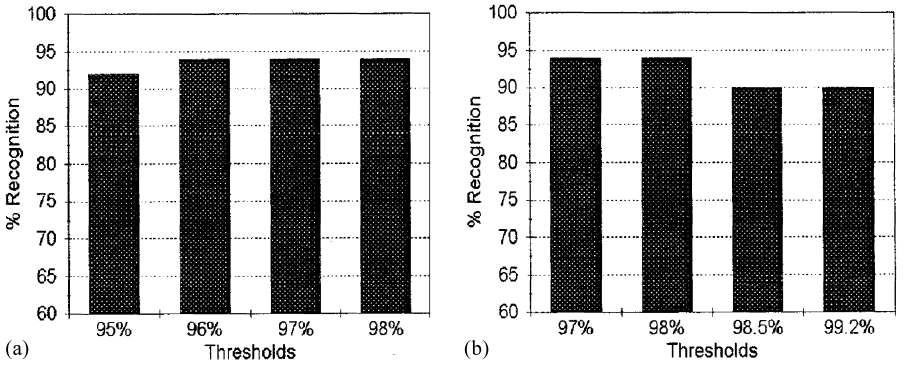

Fig. 27. Wavelet correlation classification results for binary and thinned binary prints $j = 3$. (a) Binary. (b) Thinned.

adding the newly extracted features to a training set. In such a case, the best option is probably the one nearest neighbour classifier as it needs no training and its performance tends towards the optimal Bayesian performance as the number of training samples are increased. However unless a 24 h application is needed, a neural network classifier could retrain every night. In most cases this is not required and thus the best system to use would be the probabilistic or back-propagation neural networks. The exact selection would depend on the type of features.

It was noted that although some classifiers might have provided the same percentage of correct results, the actual prints correctly or incorrectly labelled sometimes differed from one classifier to another. Thus, improved classifier performance may be obtained by using multiple classifiers and requiring the majority of them to agree on the result. This would fractionally slow down the system.

Correlation-based matching techniques were investigated to determine if a suitable verification system may be designed. The existing cross-correlation technique which selects the maximum normalised value did not provide good enough results on the damaged prints and was thus rejected. The new technique of counting the number of pixels above a certain threshold of the normalised cross-correlation function performed satisfactorily better than the maximum value criteria, but the results here were also not quite good enough for selection. Applying the position standardisation technique marginally improved the results but not enough to provide completely accurate recognition.

An improvement of the correlation technique was to cross-correlate the wavelet transforms of two prints (at a certain resolution level), normalise this cross-correlation and then count the number of pixels above a predetermined threshold. This technique (which has never been used before) performed far better than when applied to normal untransformed prints. The wavelet transform used is not too computationally expensive as long as the resolution levels are kept low. Since the binary prints operate best on a resolution level of two, this would be the logical choice for an identification system. (A suitable verification threshold may be selected for these prints). The pre-rotation and translation procedure is unnecessary to use, as a physical guide (built into the hardware) would provide a more viable alternative. However, depending on the application, this procedure may be selected for use. The cross-correlation is performed in the frequency domain to speed up the operation. If used in an identification application, this technique is only suitable for very small databases as the correlation of the test image with each image in the database must be performed. An optical or parallel system should overcome this disadvantage. Unfortunately for situations where little storage capacity is available, this technique is unsuitable as each print in the training set must be stored (actually the Fourier transform of the wavelet transform should be stored). An advantage of this method is that only one training print per class needs to be used. A more robust system may be developed where three training prints per class are used and at least two must positively confirm the identity. Of course, this technique is really only suitable for small database, fast optical systems. Issues such as computation time and storage space have already been discussed. The techniques used here have not been tested on very large databases and if such an application is required, the results would have to be re-evaluated. Obviously, the results should improve if a better optical system is available or if the database consisted only of 'good' prints.

This paper has attempted to analyse many techniques for all the stages of a recognition system. However, many more ideas and techniques are available and it would be impossible to think of all possible scenarios and deal with them. The techniques proposed are intended to cover a wide spectrum of ideas and are more than suitable for

the proposed task. With the exception of the Fourier features and the ordinary correlation technique, all the techniques proposed have previously never been applied to fingerprint recognition scenarios, and none of the techniques have been investigated before on damaged prints. Other ideas that may be investigated in the future would have to focus on speed performance and to try to reduce the number of training prints required.

References

[1] B. Sherlock, D. Monro, K. Millard, Fingerprint enhancement by directional fourier filtering, IEE Proc. Vision Image Signal Process. 141 (2) (1994) 87–94.
[2] L. O'Gorman, J. Nickerson, An approach to fingerprint filter design, Pattern Recognition 22 (1) (1989) 29–38.
[3] B. Methre, Fingerprint image analysis for automatic identification, Mach. Vision Appl. 6 (2–3) (1993) 124–139.
[4] L. Coetzee, E.C. Botha, Fingerprint recognition in low quality images, Pattern Recognition 26 (10) (1993) 1441–1460.
[5] Q. Xiao, H. Raafat, Fingerprint image postprocessing: a combined statistical and structural approach, Pattern Recognition 24 (10) (1991) 985–992.
[6] K. Moscinska, G. Tyma, Neural network based fingerprint classification, in: IEE Conference Publication, number 372, IEE, Stevenage, England, 1993, pp. 229–232.
[7] S. Leung, W. Leurig, W. Lati, A. Luk, Fingerprint recognition using neural network, in: Proceedings of the 1991 Workshop on Neural Networks for Signal Processing, IEEE Communications Society, 1991, pp. 226–235.
[8] D. Weber, A cost effective fingerprint verification algorithm for commercial applications, in: Proceedings of the S.A. Symposium on Communications and Signal Processing, SAIEEE, 1992, pp. 99–104.
[9] A. Brink, Grey-level thresholding of images using a correlation criterion, Pattern Recognition Lett. 9 (1989) 335–341.
[10] Y. Chen, W. Hsu, A modified fast parallel algorithm for thinning digital patterns, Pattern Recognition Lett. 7 (1988) 99–106.
[11] M. Kawashima, K. Kiji, Personal identification by fingerprint or palmprint, Inform. Process. 25 (1984) 599–605.
[12] F. Pernus, S. Kovacic, L. Gyergyek, Minutiae based fingerprint recognition, in: Proceedings of the 5Th International Conference on Pattern Recognition, 1980, pp. 1380–1382.
[13] S. Leung, A. Luk, W. Suen, C. Cheng, A low cost fingerprint recognition subsystem for security systems, Vol. I., AMSE Press, Brighton, UK, 1989, pp. 221–232.
[14] W. LeRoux, E. Botha, Fingerprint based security lock, in: Proceedings of the 5th S.A. Workshop on Pattern Recognition, 1994.
[15] C. Arcelli, G. Baja, A width-independent fast thinning algorithm, IEEE Trans. Pattern Anal. Mach. Intcll. PAMI 7 (4) (1985) 463–474.
[16] D. Glover, An optical fourier/electronic neurocomputer automated inspection system, in: International Conference on Neural Networks, San Diego, 1988, pp. 1-569–1-576.
[17] A.K. Rosenfield, A. Kak, Digital Picture Processing, Academic Press, New York, 1976.
[18] R. Duda, P. Hart, Pattern Classificatz'on and Scene Analysis, Wiley, New York, 1973.
[19] C. Chen, Statistical Pattern Recognition, Hayden Book Company, Inc., New Jersey, 1973.
[20] D. Specht, Probabilistic neural networks, Neural Nctworks 3 (1990) 109–118.
[21] J. Starck, F. Murtagh, A. Bijaoui, Image Processing and Data Analysis: The Multiscale Approach, CUP, 1998.

About the Author—ANDREW JOHN WILLIS graduated in Theoretical Physics from Cambridge University UK and went on to postgraduate studies at London University in Solid State Electronics. His first research position was at the Council for Scientific Research in South Africa where his work on the fabrication of microwave devices led to a Ph.D. in 1987. Later as a Research Associate at University College London, he worked on radar signal processing for the space programme and in 1991 accepted a teaching position at the University of Witwatersrand Johannesburg. Recently Dr Willis moved to Canada where he is a consultant to General Electric. Dr Willis has published over 50 papers and is member of IEEE/ IEE. His interests are in statistical signal processing, pattern recognition, telecommunications and recently power systems.